Communications in Nonlinear Science and Numerical Simulation 106 (2022) 106107

Contents lists available at ScienceDirect

Communications in Nonlinear Science and Numerical Simulation

journal homepage: www.elsevier.com/locate/cnsns

Research paper

A thermodynamic analysis of end-directed particle flocking in chemical systems

B. De Bari [a], J. Dixon [a], J. Pateras [b,d], J. Rusling [c,d,e,f], J. Satterwhite-Warden [c], A. Vaidya [g,h,*]

[a] CESPA and Department of Psychology, University of Connecticut, Storrs, CT 06269, USA
[b] Department of Computer Science, Virginia Commonwealth University, Richmond, VA 23220, USA
[c] Department of Chemistry (U-3060), University of Connecticut, Storrs, CT 06269, USA
[d] Institute of Material Science, Storrs, CT 06269, USA
[e] Department of Surgery and Neag Cancer Center, UConn Health, Farmington, CT 06032, USA
[f] School of Chemistry, National University of Ireland at Galway, Ireland
[g] Complex Fluids Lab and Department of Mathematics, Montclair State University, Montclair, NJ 07043, USA
[h] Department of Physics and Astronomy, Montclair State University, Montclair, NJ 07043, USA

ARTICLE INFO

Article history:
Received 23 June 2021
Received in revised form 20 October 2021
Accepted 5 November 2021
Available online 9 November 2021

Keywords:
Self-organization
Flocking
End-directedness
Mass-action
Free energy

ABSTRACT

We discuss the thermodynamics behind self-organizing Benzoquinone (BQ) particles on air–water interface. Experiments (Satterwhite-Warden et al., 2015; Chen et al., 2019; Satterwhite-Warden et al., 2019) reveal that BQ particles undergo rapid transient flocking behavior as they move around on the liquid surface. Flocks are seen to vary in size and their formation and stability appears to be dependent upon their shape. It is hypothesized that self organization of particles is a result of surface tension gradients in the two dimensional liquid surface resulting from the slow dissolution of the BQ particles. The current paper uses a mass-action kinetic framework to study the flocking of particles. Two dynamical models, with and without a reservoir, are proposed and analyzed through the thermodynamic lens of free energy, which informs us about dominant and spontaneous 'reactions' or flock formations in the system. Results of the model are in good agreement with experiment, revealing that irregular shaped BQ particles do indeed show far greater propensity to form flocks compared with regularly shaped particles and validating the mass-action framework as an appropriate tool to investigate this system.

1. Introduction

This paper is devoted to the study of collective motion and self-organization in dissipative systems. Collective motion is a phenomenon displayed across all scales of living organisms, be it a flock of birds in flight, a school of fish, or a colony of ants or bacteria. Interestingly, we have been able to observe several similar qualitative features in the laboratory, under appropriate conditions, in non-living systems, allowing us to identify generic conditions for collective behavior in its many forms [1]. Experimental observations of patterns and organization requires a gradient inducing system [2] which then provides an impetus for self propulsion that supports the foraging of energy from the local environment. Chemotaxis, i.e., motion in response to a chemical gradient, is a phenomenon displayed by living and non-living systems

* Corresponding author at: Complex Fluids Lab and Department of Mathematics, Montclair State University, Montclair, NJ 07043, USA.
E-mail address: vaidyaa@montclair.edu (A. Vaidya).

https://doi.org/10.1016/j.cnsns.2021.106107
1007-5704/

alike and therefore an apt way to gain better understanding about the complexity of life. While there are several different chemotactic systems, here we address the dynamics of Benzoquinone (BQ) particles on water–air interface. Recent work [3–6] on BQ particles have shown them to be interesting systems capable of revealing much about collective dynamics.

Explanations for nature's patterns have come in two forms, (i) bottom-up causal arguments, i.e., dynamical approach based on Newton's laws or variations thereof and, (ii) top-down optimality arguments founded on a non-equilibrium thermodynamic approach. There is growing evidence that most natural phenomena are far from thermodynamic equilibrium and maintained there by inherent dissipative mechanisms; therefore patterns in nature may be the result of a more fundamental and underlying thermodynamic design. Recent studies [7–13] attest to the power and significance of thermodynamic-based approaches to the investigation of complexity, self-organization and emergence, all key to the development of a 'theory of living systems'. The central idea in these studies, and the thermodynamic school of thought more broadly, is that entropy generation and free-energy consumption are inherent traits of living and non-living dissipative systems alike. Non-living self-organizing systems thus serve as practical analogues of more sophisticated biological counterparts. Other works [14] argue in favor of dynamics as a means to gain clarity about the self-organizing systems. In this paper, we approach collective motion through the combined efforts of mechanics and thermodynamics. Our assumption is that collective dynamics must necessarily be instantiated by motion and forces while the driving mechanism for this behavior is best explained through the energetics of the system, necessitating a thermodynamic approach.

The dynamics of autonomous chemical swimmers is a rapidly expanding topic of research. Many such systems are composed of solid particles of compounds (e.g., camphor, benzoquinone) floating at the air–water interface [2–6,15–18]. The dissolution or sublimation of compounds from the solid phase generates surface tension gradients that drive individual particles across the fluid surface. We have studied the dynamics of collectives of benzoquinone (BQ) particles at the air–water interface, which demonstrate a tendency to aggregate into collective assemblies of particles that we call "flocks" [3,5,19]. This flocking dynamic is hypothesized to be driven by the variation in dissolution-induced surface tension gradients. Further, we have hypothesized that this phenomenon is also driven by an intrinsic end-directedness to maximize dissipation or to maximize the rate of entropy production [5].

In prior work (discussed in greater detail in subsequent sections), our colleagues reported on the aggregation dynamics of BQ particles at the air–water interface. Experiments were conducted with two types of BQ particles, (1) symmetric, circularly shaped disks and (2) asymmetric fragments of BQ disks. The latter irregular pellets were made by breaking large BQ disks into fragments of similar surface area of the circular pellets. One remarkable observation was that the irregularly-shaped particles have a much higher tendency to aggregate into flocks than the regularly-shaped circular pellets. These flocks emerge over the course of the experiment (on the order of 10s of seconds), tend to exhibit collective motion through the dish, and may fluctuate in size and particle number. Comparable dynamics were not observed in experiments with regularly shaped circular pellets. One candidate explanation for this phenomenon appeals to the differences in interfacial-tension and mass-flow due to the difference in pellet geometry, and such an analysis is pending. Here we pursue an explanation for these differences deriving from end-directed or variational thermodynamic principles.

Non-equilibrium variational principles are highly sought-after, as they would enable predicting the time-evolution of complex open systems, from turbulent fluids to biological systems [12,20]. These include the hypotheses that systems will maximize the rate of entropy production (MEP) [12], or minimize the Gibbs free energy (MinFE) [21,22]. We have previously theorized that the flocking of BQ particles might similarly be driven by such a selection principle [5], namely MEP. It was suggested that the emergence of flocks was due to the system converging on a state with maximum rate of entropy production (MEP). REP was approximated by estimating the dissolution rate constant k for the two types of BQ particles (regular and irregular). It was observed that flocks of irregularly shaped particles had higher k values than non-flocking regular-particles, consistent with the hypothesis that flocking produces greater entropy production than not flocking. However, this result lacks an appropriate control condition, as we cannot compare the MEP between flocking and non-flocking dynamics within particle type (regular and irregular).

Herein we continue to explore explanations for the flocking phenomenon deriving from a variational principle. Using mass-action kinetics to simulate the flocking dynamics, we investigated how the change in Gibbs free energy, ΔG, related to the emergence of flocks of different sizes. From this we demonstrate that the preferred flock sizes of both regular and irregular particles tend to minimize the Gibbs free energy, consistent with a variational principle like MinFE.

2. Experiments

The experimental data reported in this study are based on experiments originally performed and reported in Satterwhite-Warden et al. [4]. This study examined the spontaneous dynamics of Benzoquinone (BQ) particles on water–air interface. The BQ particles were made in two forms, irregular and circular. The irregular particles had sharp edges and non-uniform shape while the circular particles were 3 mm disks of BQ.

2.1. Materials and methods

The experiment used 1,4-Benzoquinone (BQ), lycopodium, and sodium chloride (NaCl), all from Sigma-Aldrich. Nanopure water (18 megaohm cm) was house-distilled, and then purified by a Hydro Service and Supplies system. The BQ powder was first finely ground in a mortar and then molded into a pellet (either 3 mm diameter, 1 mm thick or 13 mm diameter, 1 mm thick) with a die set and press, either a hand press (Pike Technology, model no. 161-1100) or hydraulic press (Carver Inc., model no. 4350L) was used. Two different particle forms were implemented: circular 3 mm BQ disks or irregularly shaped and sized BQ fragments. The irregular BQ particles were made by breaking 13 mm BQ disks into pieces. The circular particles were used in the shape created by the press. All particles were lightly dusted with lycopodium powder, a hydrophobic material that helps the keep particles at the air–water interface, and thus extend the observation time of self-motion.

BQ particles were gently added to the air–water interface of aqueous 0.1 M NaCl. The aqueous medium was in a rigorously cleaned, surfactant-free glass Petri dish (90 mm diameter). This aqueous volume was selected such that BQ particles did not touch the bottom on the Petri dish. The motion of particles was recorded using a digital video camera (JVC-HD GZ-E200BU, frame rate: 30 fps). The recording was terminated when the particles dissolved or sank. Image analysis was done using ImageJ 1.41 [23]; the [x,y] coordinates for each particle for each frame were manually acquired using the MTrackJ plugin [24]. The resulting [x,y] coordinates for each trial were analyzed using the R statistical programming language [25] (see Fig. 1).

2.2. Experimental results

The images are used to define flocks of various sizes. If the centers of any two or more BQ particles are within a distance $r < r_{crit} = 125$ pixels, we define the particles to be part of a flock. In this paper, we examine six experiments corresponding to systems of size ranging from a total of 4–15 particles. Five different flock-bins are defined and labeled A–E, each flock representing a range of flock sizes defined in Table 1. Fig. 2 summarizes a significant observation for each of these systems by showcasing the average percentage distribution of each flock over the entire 100 s of observations. An emergent self-organization property in the BQ system can be stated as follows: (a) symmetric particles tend to persist as single particles or primarily as smaller flocks; (b) in irregularly shaped particles, the system shows a reduction in smaller flocks (A,B) and a noticeable increase in larger flocks (D,E). Quantitative definitions of 'small' and 'large' flocks cannot be given in general and are sensitive to the system under discussion. For instance, in the 8-particle system, in moving from regular to irregular particles we see the flocks A,B enlarge to include a significantly larger percentage of flocks C and D.[1]

3. Modeling setup

We employ a mass-action based framework to model the interactions between 'particles' on an air–fluid boundary as they form 'flocks' or groups of particles. Distinct from experiments, the model treats the particles as continuous systems and their interaction as discrete event, determined by rate constants. The parameters α_i and β_i with $1 < i < 10$ are the rates of associations and dissociations of the flocks respectively and are obtained by performing curvefits to experimental data. While the model is formulated in general, the distinction between the two types, regularly shaped versus irregularly shaped ones are made by rate constants which are obtained from fits to experimental data. These constants will be used as the groundwork for a network thermodynamic analysis of the mass transfer modeling flock formation. The constants $\alpha_1 - \alpha_{10}$ represent *cohesion* flocking tendencies while $\beta_1 - \beta_{10}$, all backward rates, represent *separation* tendencies.

In the interest of reducing the computational complexity of the problem, we define five bins as described in the previous section, denoted A to E, to study flocking dynamics. The choice of bins depend on the total number of particles in the system, for which a representative value is assumed based on the experiments. Our computations are focused on two systems, one containing 12 individual particles and the other containing 16 particles.[2] Table 1 shows the binning structure for these two cases, with the representative value for each bin.

The difficulty in obtaining aggregation/separation data for each flock size, requires some parameter reduction. In order to match the order of our input data (5 flock bins) to the output of our curve fit we make the following assumptions: (a) all rates into flock $A := \beta_1$; (b) all rates into flock $B := \alpha_1$; (c) all rates into flock $C := \alpha_2$; (d) all rates into flock $D := \alpha_3$ and (e) all rates into flock $E := \alpha_4$. This assumption allows us to reduce the number of parameters from 12 to 16. This amounts to the assumptions that

$$\beta_1 = \beta_5 = \beta_6 = \beta_7 \tag{1}$$

$$\alpha_1 = \beta_2 = \beta_8 = \beta_9 \tag{2}$$

$$\alpha_2 = \alpha_5 = \beta_3 = \beta_{10} \tag{3}$$

$$\alpha_3 = \alpha_6 = \alpha_8 = \beta_4 \tag{4}$$

$$\alpha_4 = \alpha_7 = \alpha_9 = \alpha_{10} \tag{5}$$

where each of the rate constants have units of 1/s.

[1] It is to be noted that in the 8-particle and 10-particle system, D represents the largest flock in accordance with the definition of Table 1.

[2] We shall henceforth describe this as '15-particle system' to maintain consistency with experiments.

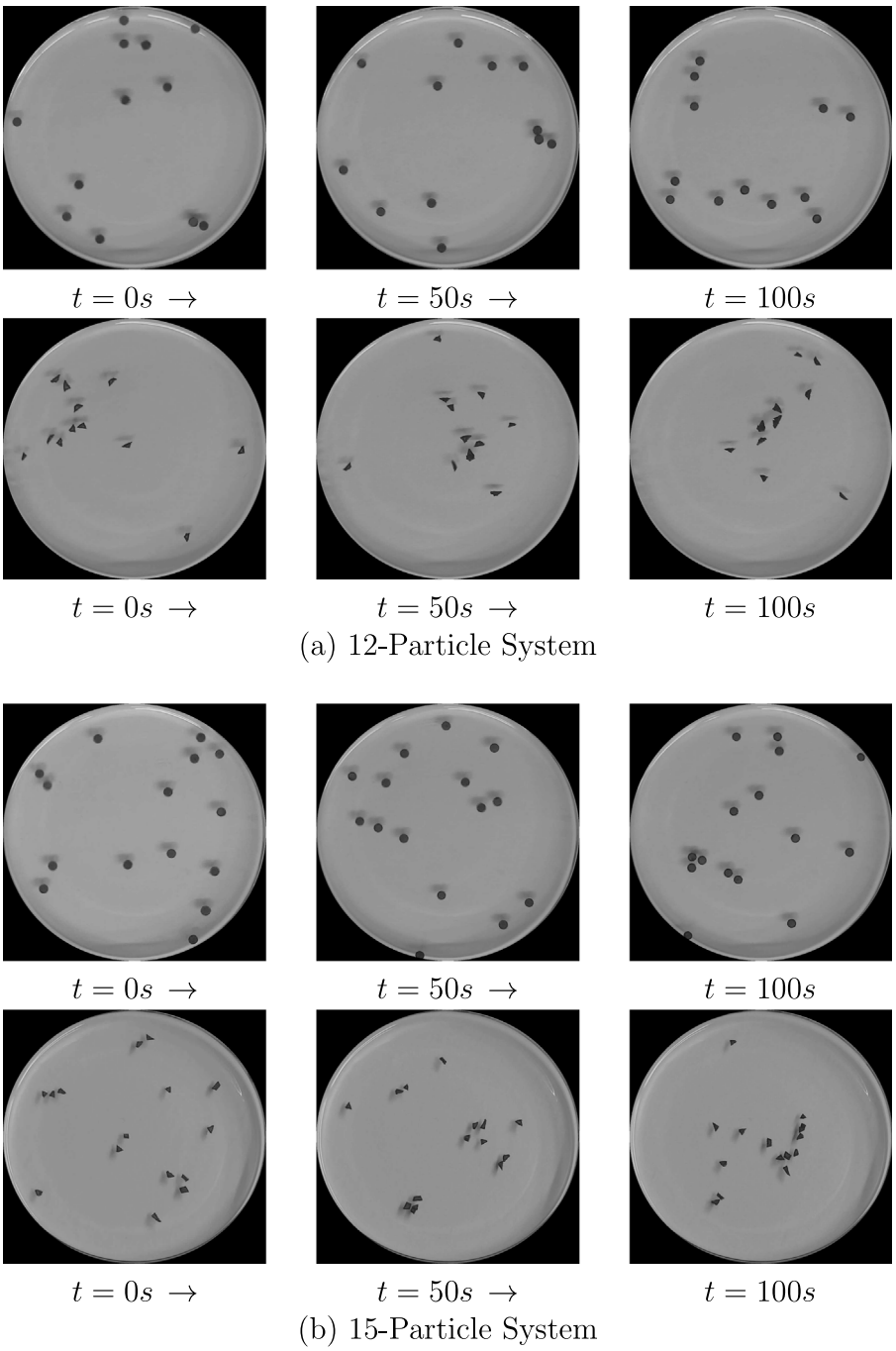

Fig. 1. This figure shows time lapse images of flocking dynamics for the (a) 12 particle and (b) 15 particle BQ systems at three different times. The top row for each of the two cases shows disk shaped particles while the second row corresponds to irregularly shaped particles.

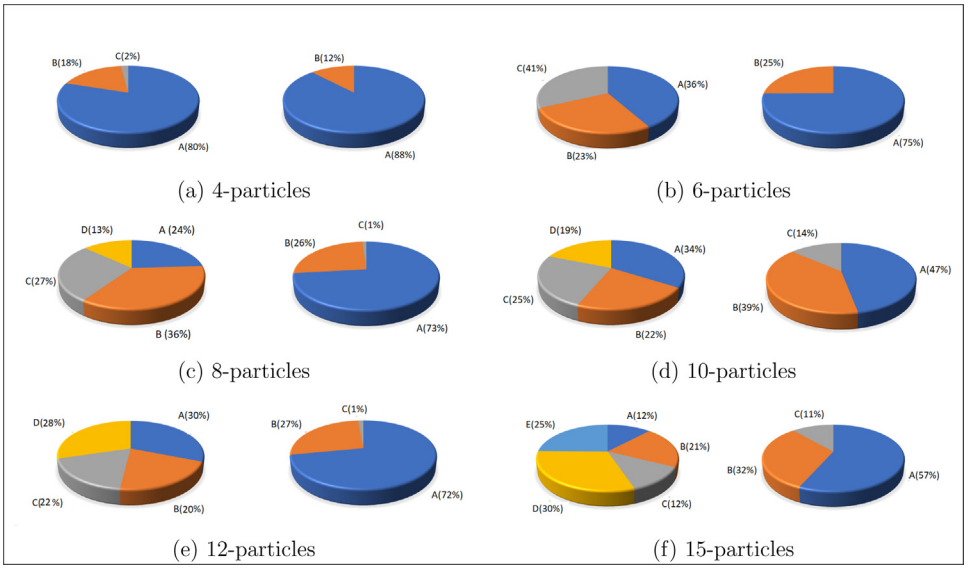

Fig. 2. This figure shows the average distribution of particles of various sizes over an entire experiment showing the propensity of the system to form specific flocks. The panels (a)–(f) represent different system sizes, ranging from (a) 4 particles to (e) 15-particles. In each case, the panel on the left corresponds to irregularly shaped particles while the one on the right corresponds to regular, disk shaped particles. The binning of flocks is described in Table 1. The legends reveal the fraction of the solid area covered by each flock. The comparison between disks and irregular particles in each panel reveals a clearly shift towards larger flocks, on average.

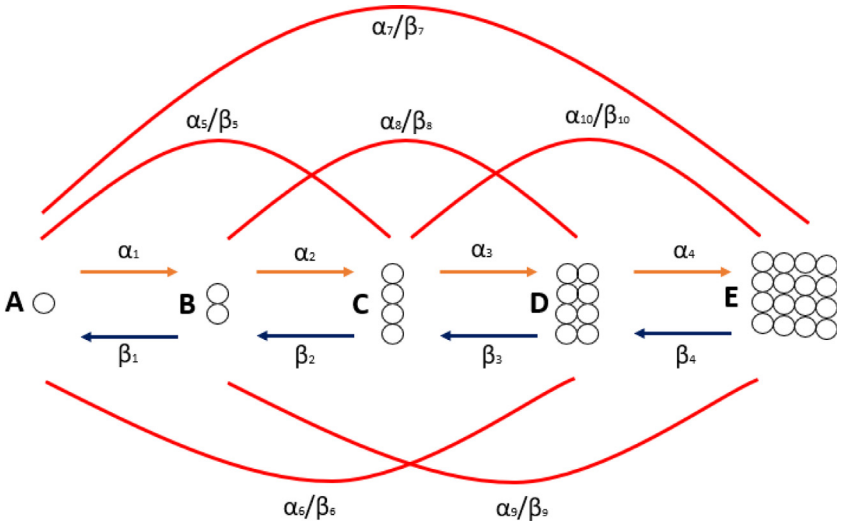

Fig. 3. The figure shows a cartoon of the modeling scheme depicting the various pathways between the five flocking bins $A-E$ and their reaction rates.

3.1. Mass action equations

Fig. 3 provides a schematic of the aggregation model adopted here. The mass-action based, coupled dynamical system for the 15 particle system is given below for a representative size corresponding to each bin (A-1; B-2; C-4, D-8; E-16). This model employs the five rate constants under the assumption described earlier.[3]

$$\begin{aligned}\frac{dA}{dt} &= \beta_1(2B + 4C + 8D + 16E) - (2\alpha_1 A^2 + 4\alpha_2 A^4 + 8\alpha_3 A^8 + 16\alpha_4 A^{16}) \\ &= \mathcal{F}_A(A, B, C, D, E) \end{aligned} \tag{6}$$

[3] A similar system, derived for the 12 particle modeled is shown in Appendix A.

Table 1
The table shows the range of each flock for the model system ranging in size from 4 to 16-particles. For sake of convenience, a representative size for each bin is chosen in the computations which is the underlined number. It is to be noted here that while the experiments referenced in the paper correspond to a 12-particle and 15-particle system, we approximate the latter with 16-particles for consistency with theory. However, in the rest of this paper we shall use '15-particle system' to describe this scenario to maintain consistency with experiments.

Bins # Particles	A	B	C	D	E
4	1	(2,3)	(4)	–	–
6	1	(2,3)	(4,5,6)	–	–
8	1	(2,3)	(4,5,6)	(7,8)	–
10	1	(2,3)	(4,5,6)	(7,8,9,10)	–
12[a]	1	(2,3)	(4,5,6)	(7,8,9)	(10,11,12)
16	1	(2,3)	(4,5,6)	(7,8,9,10)	(11,12,13,14,15,16)

[a]See Appendix A for details of the relevant equations for this system.

$$\frac{dB}{dt} = \alpha_1(A^2 + 2C + 4D + 8E) - (\beta_1 B + 2\alpha_2 B^2 + 4\alpha_3 B^4 + 8\alpha_4 B^8) = \mathcal{F}_B(A, B, C, D, E) \tag{7}$$

$$\frac{dC}{dt} = \alpha_2(A^4 + B^2 + 2D + 4E) - (\beta_1 C + \alpha_1 C + 2\alpha_3 C^2 + 4\alpha_4 C^4) = \mathcal{F}_C(A, B, C, D, E) \tag{8}$$

$$\frac{dD}{dt} = \alpha_3(A^8 + B^4 + C^2 + 2E) - (\beta_1 D + \alpha_1 D + \alpha_2 D + 2\alpha_4 D^2) = \mathcal{F}_D(A, B, C, D, E) \tag{9}$$

$$\frac{dE}{dt} = \alpha_4(A^{16} + B^8 + C^4 + D^2) - (\beta_1 + \alpha_1 + \alpha_2 + \alpha_3)E = \mathcal{F}_E(A, B, C, D, E) \tag{10}$$

In order to examine the stability of flock formation within our model we examine the change in free energy, ΔG, associated with the mass transfer into each flock bin. ΔG for a reaction pathway is a physically apt way to examine the dominant stable reaction fluxes and forces in the system [22]. In equilibrium, Gibbs free energy is given by the expression ΔG_0 which is defined in terms of the equilibrium constant as $\Delta G_0 = -RT \ln K_{eq}$. However, the free energy can be applied to time-dependent and out of thermodynamic situations in terms of the chemical affinity of the reaction and expressed as

$$\Delta G = \Delta G_0 + \bar{\Delta G} \tag{11}$$

where $\bar{\Delta G} = RT \ln\left(R_f/R_r\right)$, R_f, R_r are the forward and reverse reactions rates respectively and R and T correspond to the Rydberg constant and ambient temperature of the system. It is the second term here which is time dependent and determines the overall direction of the reaction. More specifically, it is seen in our problem that the expression for free energy can be written as

$$\Delta G = -RT \ln K_{eq} + \bar{\Delta G}.$$

Note that a negative ΔG is indicative of a spontaneous (or stable) reaction while a positive ΔG implies that the particular reaction requires added energy to occur [22]. We point to the following possibilities:

1. When $0 < \bar{\Delta G} < \Delta G_0$ or $0 > \Delta G_0 > \bar{\Delta G}$ and $\lim_{t\to\infty} \bar{\Delta G} = |\Delta G_0|$, the net free energy of the system, $\Delta G \leq 0$ for $t \geq 0$, therefore supporting the reaction promoting the formation of the products.
2. Similarly, in the case, where $0 > \bar{\Delta G} > \Delta G_0$ or $0 < \Delta G_0 < \bar{\Delta G}$ and $\lim_{t\to\infty} \bar{\Delta G} = |\Delta G_0|$, then $\Delta G \geq 0$ for $t \geq 0$ promoting the formation of the reactants.

The objective of this paper is to investigate the sign of the free energy for reactions pertaining to formation of specific flocks.

Based on our earlier assumption of isomorphic reaction rates, there are several ways to form any of the A to E flocks but only one way to dissociate. The expressions for various free energies associated with the formation of each species is given by the equations below. Note that $\bar{\Delta G_X}$, i.e. the free energy for net formation/depletion of flock X, where $X = A$ to E are given by:

$$\bar{\Delta G_A} = RT\, ln\left(\frac{\alpha_1 B^{\frac{1}{2}} \alpha_2 C^{\frac{1}{4}} \alpha_3 D^{\frac{1}{8}} \alpha_4 E^{\frac{1}{16}}}{\beta_1^4 A^4}\right) \tag{12}$$

$$\bar{\Delta G_B} = RT\, ln\left(\frac{\beta_1 A^2 \alpha_2 C^{\frac{1}{2}} \alpha_3 D^{\frac{1}{2}} \alpha_4 E^{\frac{1}{8}}}{\alpha_1^4 B^4}\right) \tag{13}$$

$$\bar{\Delta G_C} = RT\, ln\left(\frac{\beta_1 A^4 \alpha_1 B^2 \alpha_3 D^{\frac{1}{2}} \alpha_4 E^{\frac{1}{4}}}{\alpha_2^4 C^4}\right) \tag{14}$$

$$\Delta\bar{G}_D = RT\,ln\left(\frac{\beta_1 A^8 \alpha_1 B^4 \alpha_2 C^2 \alpha_4 E^{\frac{1}{2}}}{\alpha_3^4 D^4}\right) \tag{15}$$

$$\Delta\bar{G}_E = RT\,ln\left(\frac{\beta_1 A^{16} \alpha_1 B^8 \alpha_2 C^4 \alpha_3 D^2}{\alpha_4^4 E^4}\right) \tag{16}$$

The free energy of a chemical reaction (i.e. the affinity or chemical forces of the reaction) in the case of equilibrium or non-equilibrium (near or far from equilibrium) can be expressed as function of chemical potential, denoted μ (see for instance [22]). So for instance, the Gibbs energy for the reactions $X \rightarrow Y$ and $Y \rightarrow Z$ can be expressed as

$$\Delta G_{XY} = \mu_X - \mu_Y \tag{17}$$

$$\Delta G_{YZ} = \mu_Y - \mu_Z \tag{18}$$

As a result,

$$\Delta G_{XZ} = \mu_X - \mu_Z = (\mu_X - \mu_Y) + (\mu_Y - \mu_Z) = \Delta G_{XY} + \Delta G_{YZ} \tag{19}$$

Therefore the Gibbs energy possesses an additive property, which is utilized in the theoretical computations of $\Delta\bar{G}_A - \Delta\bar{G}_E$ above, each containing the sum of contributions from different pathways identified in the Fig. 3. The linear superposition rule is invalid when computing the rate of entropy production (σ) in a non-equilibrium system, where σ is written as a product of the reaction fluxes and forces (or affinities) [22]. The non-equilibrium regime of a physical system is not always easily characterized and quantified, they key to which may be the identification of a key parameter which controls the extent of departure from thermal equilibrium [9]. In the absence of this feature, especially in chemical systems, it is meaningful to consider a thermodynamic quantity that is free of this constraint. Due to the nonlinear nature of the expression of σ, superposition breaks down when the system is far from equilibrium. However, it is generally valid in the case of free energy, which has been exploited in this problem.

3.2. Model 2: Flocking dynamics with sink

Our second model builds upon the model 1 Eqs. (10) by accounting for the dissolution of the particles into the environment (or sink) and also features concentration dependence. The dissolution is an irreversible, one way reaction, at rate k, and the concentration of particles in the sink, denoted A', is determined by the disequilibrium of flock concentration between the system and the sink. The complexity of the model system comes from the fact that the reaction rates in the BQ-environment system are dependent on the difference in concentration between the two compartments (denoted $\Delta\phi$). The flocking and dissolution into the sink continue until $\Delta\phi \rightarrow 0$. This model permits confirmation of the results of model 1 under more realistic conditions including exploration of the impact of (a) dissolution rate k, (b) surface tension gradient, which is related to concentration difference $\Delta\phi$ and (c) initial concentrations of the two compartments, upon the flocking dynamics. To be noted is that the rate of dissolution is independent of the flock itself.

The governing equations for the 15 particle system can be written as:

$$\frac{dA}{dt} = \Delta\phi\,(\mathcal{F}_A(A,B,C,D,E) - kA) \tag{20}$$

$$\frac{dB}{dt} = \Delta\phi\,(\mathcal{F}_B(A,B,C,D,E) - kB) \tag{21}$$

$$\frac{dC}{dt} = \Delta\phi\,(\mathcal{F}_C(A,B,C,D,E) - kC) \tag{22}$$

$$\frac{dD}{dt} = \Delta\phi\,(\mathcal{F}_D(A,B,C,D,E) - kD) \tag{23}$$

$$\frac{dE}{dt} = \Delta\phi\,(\mathcal{F}_E(A,B,C,D,E) - kE) \tag{24}$$

$$\frac{dA'}{dt} = k\Delta\phi\,(A+B+C+D+E) \tag{25}$$

where $\Delta\phi = (A+B+C+D+E) - A'$. As $\Delta\phi \rightarrow 0$, the right sides of Eqs. (20)–(25) vanish and the system reaches steady state. Also, if the dissolution rate $k \rightarrow 0$, A' becomes irrelevant and the system of equations revert back to the original model, i.e. the one without the sink. Initial conditions assumed for our investigations are based on experiments.

4. Results

The rate constants $\alpha_1 - \alpha_4$ and β_1 were obtained from fitting model equations (6)–(10). Rate constants are calculated by the method of least squares with the MATLAB *lsqcurvefit* function. We solve for rate constants r in the governing equation F by finding the parameters which solve the problem: $min_r \|F(r, t_{data}) - y_{data}\|_2^2 = min_r \sum_i (F(r, t_{data_i}) - y_{data_i})^2$ where y_{data} is the experimentally observed flock number at each instance of time. Experimental data is preconditioned by performing

Table 2
This table shows the values of the five primary rate constants obtained from fitting data from 12 and 15 particle experiments to the mode 1.

Rate Constants # Flock Size & Type	α_1	α_2	α_3	α_4	β_1
12-Regular	12.12097	0.95147	1.01760	0.72269	12.98397
12-Irregular	0.06961	0.00852	0.00003	0.00000	0.85915
15-Regular	53.21555	5.26241	8.61908	10.02046	35.29300
15-Irregular	0.30348	0.10051	0.08829	0.01088	1.00464

a polynomial fit employing the MATLAB *polyfit* function, thus avoiding the computational trouble of many discontinuities and zero-valued inputs. The same constants were used in the study of Eqs. (20)–(25). The dynamical equations were numerically solved using a six-stage, fifth-order Runge–Kutta method via the Matlab *ode*45 function. In such a largely interdependent, non-linear system many equilibria are expected. Thus we use MATLAB function *fsolve* to determine the nearest equilibrium to an initial guess informed by our numerical solutions. When compared, our methods show a less than 0.1% error with respect to the *fsolve* output for each flock size estimation. Table 2 provides the fitted constants for various scenarios. Additionally, the dissolution rate k was estimated from experiments as the reciprocal of the time taken to reach steady state. On average the value of $k \approx 0.01$. Table 3 shows the average value of each flock number, the corresponding steady state flock number obtained by our model with the rates provided in Table 2, and relevant statistical values. We exhibit confidence in our fitted values by their ability to capture the overall behavior of the flocking system by examining the bin average absolute error (expressed in units of particles) in context of the data average standard deviation in each bin. If the absolute error in predicting our bin sizes is less than, or relatively close to the standard deviation of the experimental data, we assume reasonable confidence in our parameter fits (see Table 2).

The concentrations of the various flocks were used to compute the steady and time dependent free energy values for flock formation. Fig. 4(a) and (b) shows the steady $\bar{\Delta G}_i$ values ($i = A, B, C, D, E$) for the 15 and 12 flock cases. Clearly, in the case of the irregularly shaped BQ particles, the values of ΔG are negative in the case of larger flocks showing a preference for flocks C, D and E with the most spontaneous being flock E. In the case of the regularly shaped particles, the intermediate flock size (i.e. flock C) appears to be the most preferred one. The computations suggest that regardless of the total number of particles, irregularly shaped particles form large flocks more spontaneously than regularly shaped particles and are in strong qualitative agreement with experimental observations.

Eqs. (20)–(25) of model 2 are also solved and respective free energies are compared in the presence of a sink. Figs. 4(c)–(e) shows the results of the time dependent ΔG calculations for the 12 and 15-particle system, including the sink. Spontaneity of the reaction requires $\Delta G < 0$ and this requirement helps put a constraint on the parameter k. For $0 < k < 0.877$, $\Delta G_{sink} < 0$. This agrees with the physical actualization of constant particle dissolution towards saturation. The value of k assumed in this study ($k = 0.01$) falls well within this range. Overall, the results for this model are also in good qualitative agreement with observations. As seen earlier, at longer times, $\bar{\Delta G}_E < \bar{\Delta G}_D < \bar{\Delta G}_C < 0$ dominate the irregular system while the regular particles lean in the direction of intermediate to smaller particles with $\bar{\Delta G}_C < 0$, with the free energies for the other flocks being positive for all times computed.

The solution of the governing equations also allow for computation of the area which each flock occupies when our model reaches steady state. The area of each flock is given by the product of the estimated particle area and number (or concentration) of each flock derived from the computations. The characteristic area is chosen to be the size of one A-flock at initial time which is assumed to be unity, without loss of generality. For the 15 particle system we can see that the irregularly shaped particles form in such a way as to maximize the area allocated to E-flocks, while the regularly shaped particles clearly do not maximize large flocks through their interactions. Irregular particles, once again show a clear preference for larger flocks, especially in the 15 particle case, while the smaller D-flock dominates in area for the regularly shaped particles. The 12 particle case only shows a mild preference for E flock.

5. Discussion

The primary contribution of this paper is the mapping of experimental observations on flocking of BQ particles [3–5] to a mathematical model via mass-action kinetics. While the experimental system is discrete, yet, the continuous dynamical model is able to capture the essential characteristics of this system. There are good reasons to use such a dynamical model to help explain flocking behavior: (a) collective motion and self-organization in living and non-living systems are driven by chemical gradients, therefore a reduction of the system to a set of interrelated chemical reactions is a good first approximation, (b) such a model affords a thermodynamic perspective as well through the formulation of free energy (ΔG), which is key to this analysis. Satterwhite-Warden et al. hypothesize that [5], "The flock responds to changes in its local environment as it forages for interfacial free energy". A free energy based analysis is therefore central to understanding self organizing behavior, as previously noticed and as the results of this study clearly indicate.

Some recent work in the area of protein aggregation has shown such models to be particularly useful when examining competitive self-assembly scenarios [21] and the problem treated here is not so dissimilar despite the assumptions of continuity, for this discrete system. One added advantage of this analysis which is yet to be fully exploited is the

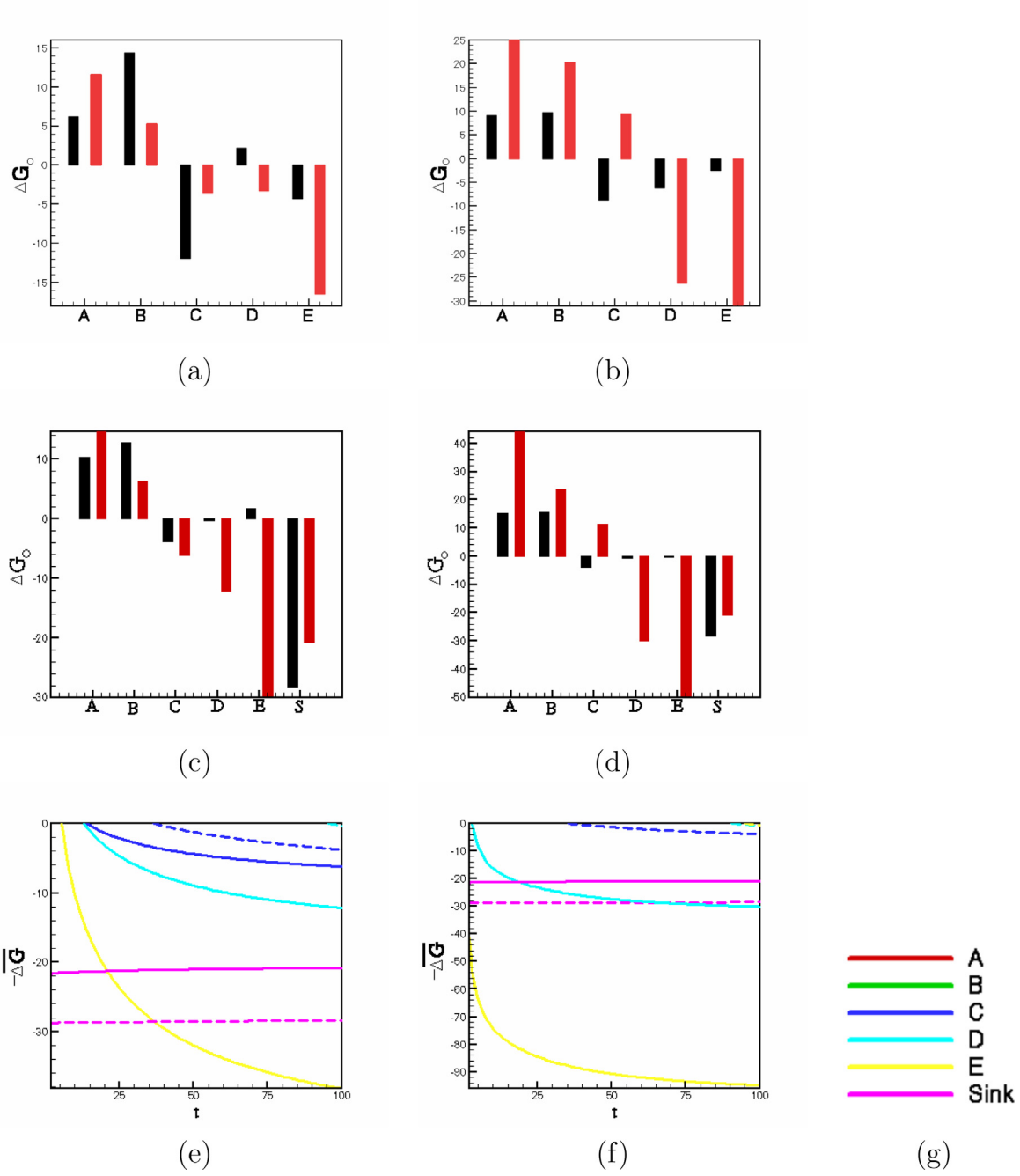

Fig. 4. This figure shows the results of free energy calculations for 15 (panel a) and 12 (panel b) particle system for model 1 while (c) and (d) show the same for model 2. Here the black bars represent the disk shaped particles, while red bars represents the irregularly shaped. No matter the size of the system, ΔG is able to clearly distinguish between the dynamics of regular and irregular particles. In the case of irregular particles, larger flocks show greater propensity to display negative values while in the case of regularly shaped particles, the intermediate flocks reveal the greatest probability to occur. The panels (e) and (f) show the time dependent change in the free energy for each flock for model 2 for the 15 particle and 12 particle system respectively. The legend shows the color associations with the flock bin and the solid versus dashed curves, help distinguish between irregular and regular shapes. This final graph shows only those flocks for which ΔG is negative.

potential to examine thermodynamic aspects beyond free energy. Self organization is inherently an outcome of the evolving energies and entropy in dissipative systems [12,22] and this system lends itself quite well to examining questions about the merits of the maximum entropy production principle which will be studied in the future. On the flip side, a problem with this approach is its reduced complexity. Binning the flocking system forces a selective organizational

structure for computational convenience which contributes to errors. However, our calculations show that the assumption of continuity through the mass action model and binning results in deviations between 1%–13% in the total number of particles, depending on the particular system. However, the model does a good job of satisfying mass conversation to within 2.8% for all systems, the error coming from variability within each bin. Therefore the results and comparison must be deemed acceptable in an average sense.

The significance of particle shape in self organization and pattern selection has been discussed in earlier works (see [8,13,26,27] and references therein). Accordingly, shapes can induce asymmetries in the surrounding medium, driving particles faster and increasing opportunities for collision. The nonlinearity of the model equations prevents us from gaining insights into the reasons behind observed differences in experiments and theory between the regular disks and irregular particles. According to [5], "However, we suspect that irregular BQ fragments elicit larger interfacial free energy differences near particle points and edges, since dissolution at such points is faster than at smooth regions of a particle. This creates a greater local driving force for particles to cooperate". The Table 2 hints at the possibility of the rate constants having something to do with this in our theoretical model but a simpler model can provide more meaningful insights into this difference. For sake of convenience we take a reduced 2-Bin system: $A \leftrightarrow B$ with constants β_1 (into A) and α_1(into B). In the framework of model 2, assuming A corresponds to an individual particle and B to a flock of size 2, this system amounts to

$$\frac{dA}{dt} = \Delta\phi\left(2\beta_1 B - 2\alpha_1 A^2 - kA\right) \tag{26}$$

$$\frac{dB}{dt} = \Delta\phi\left(\alpha_1 A^2 - \beta_1 B - kB\right) \tag{27}$$

$$\frac{dA'}{dt} = k\Delta\phi\,(A + B) \tag{28}$$

Equilibrium conditions[4] for the system require

$$A_\infty = \frac{1}{2\alpha_1}\left(-k + \sqrt{k^2 - 4\alpha_1(k - \beta_1)B_\infty}\right) \tag{29}$$

disregarding the added constraint $\Delta\phi$. Eq. (29) can now be used to examine conditions under which larger flocks would dominate, i.e. $B_\infty > A_\infty$, which upon some manipulation yields the inequality

$$\beta_1 < \alpha_1 B_\infty + 8k. \tag{30}$$

This equation clearly shows that there are thresholds on the system parameters which can push the outcomes towards formation of larger or smaller flocks. A similar analysis is very difficult to perform for larger systems like the ones discussed in this paper, which is why we rely on numerics for the 5-bin models. However Eq. (30) provides clear demarcating characteristics which determine the outcome of BQ particle flocking as a result of their shape. To compare this with model 1, we take the limiting case of $k \to 0$ in Eq. (30), which yields $\beta_1 < \alpha_1 B_\infty$. A comparison of the effectiveness of the second model, compared to the first will need to be made on the basis of a comparison against the experimental observations. In this regard, Fig. 4 is revealing; it shows the model 2 to be qualitatively more compatible with experiments in showing $\bar{\Delta G_E}$ and its corresponding value of ΔG_E to be far more negative than the free energies for other flocks. A theoretical calculation of flock areas is also made and shown in Fig. 5.[5] The pie charts of flock areas, based on the equilibrium configurations, are shown in the panels (c) and (d) of this figure and correspond to the 15 particle and 12 particle systems respectively. The former, corresponding to 15 particle systems matches very well with experiments and shows far greater proclivity for large flocks in the irregular case than for disks. There is a slight increase in the area of the E flock for the 12 particle system but the results are less conclusive which can be attributed to errors from the assumptions made for the model parameters, including the dissolution constant.

While this approach has not previously been implemented in the context of chemically induced flocking, the modeling effort by Soh, Bishop and Gryzbowski [16] on the self propulsion and organization of camphor particles merits mention. The authors employ the coupling of the two dimensional Navier Stokes equations with the diffusion equation to model the dynamics, where the diffusion of camphor into the surrounding fluid, results in a surface tension gradient, thereby causing a (Marangoni) flow which moves the camphor particles, further disrupting the surface tension distribution. It is likely that a very similar explanation is appropriate for the BQ system which operates on similar physico-chemical principles, some of which are implicitly assumed in our own model. A particularly interesting observation that emerge in the camphor system, which need to be investigated for BQ particles in the future is the existence of a critical mass above which self-organization emerges. .

[4] Equilibrium can be obtained by solving for the simultaneous zeros of Eqs. (26)–(28).

[5] This calculation is performed for model 1. The model 2 assumes a simplistic, uniform dissolution mechanism resulting in an increasing contribution to the sink with flock size. This impacts the calculation of flock area and makes it difficult to make appropriate comparisons. We therefore take the model 1 to be more meaningful in this regard.

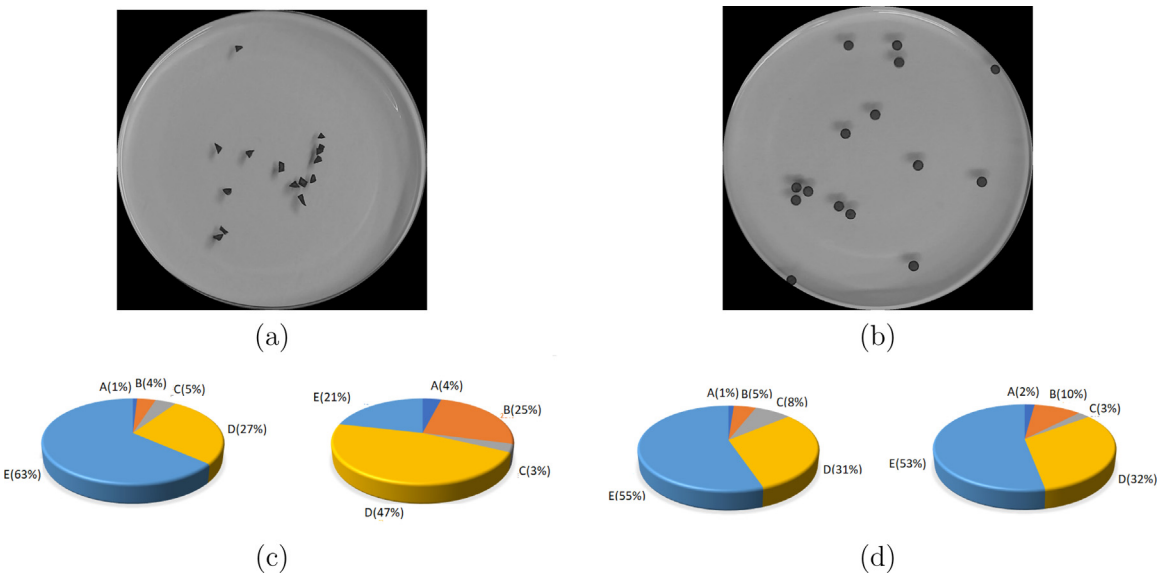

Fig. 5. The panels (a) and (b) show the equilibrium states for different shaped 15 particle system while panels (d) and (e) reveal theoretical calculations of the solid area distribution by the various flocks, with (c) corresponding to 15 particles and (d) to 12 particles. The panels (c) and (d) should be compared against similar experimentally determined profiles in Fig. 2.

6. Conclusion

One of the central quests of physics is the explanation of emergent patterns in nature. In trying to understand living systems, perhaps simplistically, we characterize 'life' as an emergent characteristic of a chemical system. Emergence can be defined as [28] "...the arising of novel and coherent structures, patterns and properties during the process of self-organization in complex systems" which are ubiquitous and independent of scale. Therefore self-organizing flocking patterns that occur in the BQ system that we study, could lead us towards the development of a theoretical framework for life itself, as is the expectation in much of the work on complexity and self-organization [14]. Our mass-action based dynamics, accompanied by a thermodynamic based analysis is worthy of further pursuit as it captures interesting characteristics of the system observed in experiments. What is lacking in this analysis is a proper accounting of the surrounding fluid environment which is an essential player in the entire event, orchestrating the particle motion through the development of a Marangoni flow [16,26] and maintaining the surface tension gradient on the fluid surface which is the driving force for the observed pattern. A mathematical formulation containing the particles and the fluid will permit for a proper accounting of the chemical/mechanical (energetics) as well as the thermodynamic aspects (entropics) of the system. The tenets of thermodynamics, especially entropy production, are recognized as immutable laws of nature and among the most fundamental guiding principles to describe end-directed behavior [22] and must be estimated for this system to fully understand the merits of the theoretical treatment adopted here.

CRediT authorship contribution statement

B. De Bari: Conceptualized the study and came up with the plan for the investigation, Co-wrote the paper. **J. Dixon:** Conceptualized the study and came up with the plan for the investigation, Co-wrote the paper. **J. Pateras:** Conducted the computations, Co-wrote the paper. **J. Rusling:** Conducted the experiments and produced data to be compared with the theoretical model. **J. Satterwhite-Warden:** Conducted the experiments and produced data to be compared with the theoretical model. **A. Vaidya:** Conceptualized the study and came up with the plan for the investigation, Conducted the computations, Co-wrote the paper.

Declaration of competing interest

The authors declare that they have no known competing financial interests or personal relationships that could have appeared to influence the work reported in this paper.

Acknowledgments

We thank Dr. Bruce Kay and Dr. Dilip Kondepudi for helpful discussions. This work was financially supported by United States National Science Foundation's INSPIRE Track 1 Program, Grant No. BCS- 1344725. Author AV also acknowledges United States National Science Foundation Grant 1802641.

Table 3
Here we catalog the average value of the number of flocks in each bin for each experiment, and the steady state value obtained by our model when running with the rate constants shown in Table 1. BAAE is the bin average absolute error, i.e. the average error for each bin between the model and experiment. We compare this value to DASD, or the data average standard deviation, i.e. the average for each bin of the standard deviation in the number of flocks in each bin.

Flock Size	A	B	C	D	E		
12-Regular							
Avg. Obs. Flock Number	7.07	1.31	0.03	0.00	0.16		
Model SS Flock Number	1.15	1.31	0.23	0.28	0.51		
						BAAE	DASD
						2.62	2.08
12-Irregular							
Avg. Obs. Flock Number	2.97	1.00	0.43	0.36	0.16		
Model SS Flock Number	3.19	1.11	0.97	0.39	0.05		
						BAAE	DASD
						0.83	2.81
15-Regular							
Avg. Obs. Flock Number	6.69	1.91	0.33	0.00	0.16		
Model SS Flock Number	0.95	1.00	0.16	0.17	0.14		
						BAAE	DASD
						1.97	1.76
15-Irregular							
Avg. Obs. Flock Number	1.09	1.02	0.29	0.41	0.47		
Model SS Flock Number	1.28	1.21	0.52	0.66	0.43		
						BAAE	DASD
						0.80	3.55

Appendix A

The governing equations for the 12 particle system, based on mass-action principle is given by:

$$\frac{dA}{dt} = \beta_1(2B + 5C + 8D + 12E) - (2\alpha_1 A^2 + 5\alpha_2 A^5 + 8\alpha_3 A^8 + 12\alpha_4 A^{12}) \tag{31}$$

$$\frac{dB}{dt} = \alpha_1(A^2 + \frac{5}{2}C + 4D + 6E) - (\beta_1 B + \frac{5}{2}\alpha_2 B^{\frac{5}{2}} + 4\alpha_3 B^4 + 6\alpha_4 B^6) \tag{32}$$

$$\frac{dC}{dt} = \alpha_2(A^5 + B^{\frac{5}{2}} + \frac{8}{5}D + \frac{12}{5}E) - (\beta_1 C + alpha_1 C + 2\alpha_3 C^2 + \frac{12}{5}\alpha_4 C^{\frac{12}{5}}) \tag{33}$$

$$\frac{dD}{dt} = \alpha_3(A^8 + B^4 - + C^{\frac{8}{5}} + \frac{3}{2}E) - (\beta_1 D + \alpha_1 D + \alpha_2 D + \frac{3}{2}\alpha_4 D^{\frac{3}{2}}) \tag{34}$$

$$\frac{dE}{dt} = \alpha_4(A^{12} + B^6 + C^{\frac{12}{5}} + D^{\frac{3}{2}}) - (\beta_1 E + \alpha_1 E + \alpha_2 E + \alpha_3 E) \tag{35}$$

The representative size of each flock here is as follows: $A-1$, $B-2$, $C-5$, $D-8$ and $E-12$. The results of the 12-particle computations presented earlier in the paper are based on these equations.

Appendix B

See Table 3.

References

[1] Whitesides GM, Grzybowski B. Self-assembly at all scales. Science 2002;295(5564):2418–21.
[2] Altemose A, Sen A. Collective behaviour of artificial microswimmers in response to environmental conditions. Self-Organized Motion: Physicochem Des Based on Nonlinear Dyn 2018;14(250).
[3] Satterwhite-Warden JE, Kondepudi DK, Dixon JA, Rusling JF. Co-operative motion of multiple benzoquinone disks at the air–water interface. Phys Chem Chem Phys 2015;17(44):29891–8.
[4] Chen T, Kondepudi DK, Dixon JA, Rusling JF. Particle flock motion at air–water interface driven by interfacial free energy foraging. Langmuir 2019;35(34):11066–70.
[5] Satterwhite-Warden JE, Kondepudi DK, Dixon JA, Rusling JF. Thermal-and magnetic-sensitive particle flocking motion at the air–water interface. J Phys Chem B 2019;123(17):3832–40.
[6] Suematsu NJ, Miyahara Y, Matsuda Y, Nakata S. Self-motion of a benzoquinone disk coupled with a redox reaction. J Phys Chem C 2010;114(31):13340–3.
[7] Bejan A. The physics of life: The evolution of everything. St. Martin's Press; 2016.
[8] Chung BJ, McDermid K, Vaidya A. On the affordances of the MaxEP principle. Eur Phys J B 2014;87(1):1–14.
[9] Chung BJ, Ortega B, Vaidya A. Entropy production in a fluid-solid system far from thermodynamic equilibrium. Eur Phys J E 2017;40(11):1–9.
[10] Kleidon A, Malhi Y, Cox PM. Maximum entropy production in environmental and ecological systems. 2010.

[11] Dewar RC, Franklin O, Mäkelä A, McMurtrie RE, Valentine HT. Optimal function explains forest responses to global change. Bioscience 2009;59(2):127–39.
[12] Martyushev LM, Seleznev VD. Maximum entropy production principle in physics, chemistry and biology. Phys Rep 2006;426(1):1–45.
[13] Vaidya A. MaxEP and stable configurations in fluid–solid interactions. In: In beyond the Second Law. Berlin, Heidelberg: Springer; 2014, p. 257–76.
[14] Pross A. The driving force for life's emergence: kinetic and thermodynamic considerations. J Theoret Biol 2003;220(3):393–406.
[15] Schulz O, Markus M. Velocity distributions of camphor particle ensembles. J Phys Chem B 2007;111(28):8175–8.
[16] Soh S, Bishop KJ, Grzybowski BA. Dynamic self-assembly in ensembles of camphor boats. J Phys Chem B 2008;112(35):10848–53.
[17] Suematsu NJ, Tateno K, Nakata S, Nishimori H. Synchronized intermittent motion induced by the interaction between camphor disks. J Phys Soc Japan 2015;84(3):034802.
[18] Suematsu NJ, Sasaki T, Nakata S, Kitahata H. Quantitative estimation of the parameters for self-motion driven by difference in surface tension. Langmuir 2014;30(27):8101–8.
[19] Kondepudi D, Kay B, Dixon J. Dissipative structures, machines, and organisms: A perspective. Chaos 2017;27(10):104607.
[20] Martyushev LM. Maximum entropy production principle: history and current status. Phys-Usp 2021;64(6):558.
[21] Ghosh P, Pateras J, Rangachari V, Vaidya A. A network thermodynamic analysis of amyloid aggregation along competing pathways. Appl Math Comput 2021;393:125778.
[22] Kondepudi D, Prigogine I. Modern thermodynamics: From heat engines to dissipative structures. John Wiley & Sons; 2014.
[23] Schneider CA, Rasband WS, Eliceiri KW. NIH Image to ImageJ: 25 Years of image analysis. Nature Methods 2012;9(7):671–5.
[24] Meijering E, Dzyubachyk O, Smal I. Methods for cell and particle tracking. Methods Enzymol 2012;504:183–200.
[25] Core Team R. R: A language and environment for statistical computing. Vienna, Austria: R Foundation for Statistical Computing; 2017, URL https://www.R-project.org/.
[26] Fei W, Gu Y, Bishop KJ. Active colloidal particles at fluid-fluid interfaces. Current Opinion in Colloid & Interface Science 2017;32:57–68.
[27] De Bari B, Paxton A, Kondepudi DK, Kay BA, Dixon JA. Functional interdependence in coupled dissipative structures: Physical foundations of biological coordination. Entropy 2021;23(5):614.
[28] Goldstein J. Emergence as a construct: History and issues. Emergence 1999;1(1):49–72.